DEVELOPMENT OF A NEW 3D EULER-LAGRANGE MODEL FOR THE PREDICTION OF SCOUR AROUND OFFSHORE STRUCTURES

Yaru Li[1], David M. Kelly[2], Ming Li[1] , John M. Harris[2]

Numerical modelling of local scour around offshore structures has recently grown in importance with the increased deployment of offshore wind turbines. Compared to single-phase models, the multiphase approach is gaining in popularity due to its capability to better interpret the flow-sediment interaction, sediment-sediment interaction and flow-structure interaction. In Euler-Euler multiphase models, both the fluid and solid phases are treated as continuum, therefore, the fluid-particle interactions cannot be resolved naturally. Moreover, Eulerian models often struggle to model complex deformation and interface fragmentation. In contrast, in pure Lagrangian models, the inherent discrete-particle property of sediment can be better represented; however, Lagrangian models are particularly demanding on computational resource. Thus, Euler-Lagrange models provide an attractive alternative retaining the advantage of simulating the solid phase naturally while being computationally efficient. In this paper, a three-dimensional Euler-Lagrange scour model based on the open source CFD software OpenFOAM®will be presented and validated. The fluid phase is resolved by solving modified Navier-Stokes equations, which take into consideration the influence of the solid phase, i.e., the particles. The sold phase is solved using multi-phase particle-in-cell (MP-PIC) approach. The particles follow Newton's Law of Motion. The hydrodynamic performance of the model is validated against experimental measurements. The impact of steady current on scour development around cylinders is also investigated.

Keywords: hybrid Eulerian-Lagrangian model; free surface; mobile bed; MP-PIC; scour

INTRODUCTION

The presence of structures in marine environment will change the flow patterns, turbulence properties, and local sediment transport in its immediate neighbourhood, resulting in local scour and then further influence the global scour pattern. Several phenomena are usually identified during the process, such as flow contraction, a horseshoe vortex in the front of the structure, lee-wake vortices with or without vortex shedding in the rear, turbulence enhancement, wave reflection, diffraction and breaking, and etc. (Sumer and Fredsøe, 2002). These changes in the flow field can amplify the local bed shear stress and enhance sediment transport capacity and thus result in a divergence of sediment transport rate and ultimately the occurrence of scour. Scour studies in the marine environment have started with the research on benthic pipelines as they play an indispensable role in the transportation of crude oil and gas in the offshore oil industry. It has been a rather demanding task to investigate the scour process to provide guidelines and suggestions to the design and protection of the exploding expansion of pipeline networks laid in the coastal and offshore areas all over the world. Extensive studies in this area has been carried out, regarding various pipe size and pipeline lengths, in different water depth and sea bed conditions, with various installation manners and in different hydrological environment (Liang et al., 2005; Zhao and Cheng, 2010; Yeganeh-Bakhtiary et al., 2011). In recent years, as one of the widely adopted approaches for the generation of renewable energies, offshore wind farms (OWF) are being built at an unprecedented speed. So far, the total installation capacity in UK is 3.653 GW with 1,075 offshore wind turbines installed (RenewableUK). This fast developing industry has made it even more urgent to have a better understanding of the complex scour processes taking place around the turbine foundations.

Numerical modelling of local scour around offshore structures has started with single-phase models. Works based on the potential flow theory were carried out at the early stage (Mao, 1986; Li and Cheng, 1999, 2000). However, with massive assumptions and a variety of empirical sediment transport formulas, these models often fail to produce the whole picture of the sediment transport and scour process; only certain aspects of the problem, such as scour depth at the upstream side, can be predicted reasonably. Compared to single-phase models, the multiphase approach is gaining in popularity due to its capability to better interpret the flow-sediment interaction, sediment-sediment interaction and flow-structure interaction, as well as revealing potential scour mechanisms. According to the different treatment of each phase (solid and fluid), multiphase models are categorized into three catalogues: Euler-Euler models, Euler-Lagrange models and pure Lagrangian models. In Euler-Euler multiphase models, both the fluid phase and the solid phase are treated as continuum, and the continuity equations and momentum equations of both phases can be solved relatively straightforwardly in an Eulerian frame. However, the fluid-particle interactions

[1]School of Engineering, University of Liverpool, UK
[2]HR Wallingford, Oxfordshire, UK

cannot be resolved naturally, thus, they must be addressed explicitly. Moreover, as Eulerian models are typically based on cell-averaged quantities they often struggle to model complex deformation and interface fragmentation.

In contrast, in pure Lagrangian models, such as Smoothed Particle Hydrodynamics (SPH), the inherent discrete-particle property of sediment can be better represented; however, Lagrangian models are particularly demanding on computational resource.

Thus, Euler-Lagrange type models provide an attractive alternative retaining the advantage of simulating the solid phase in a natural way while being computationally efficient. In this paper, a three-dimensional Euler-Lagrange scour model based on the open source CFD software OpenFOAM®(Rusche, 2002) will be presented and validated. The impact of steady current on the scour development around horizontal pipelines will also be investigated.

NUMERICAL MODEL

Motivated by the multiphase particle-in-cell (MP-PIC) method developed at Los Alamos National Laboratory by Snider and his colleagues (Snider et al., June, 1997), a new three-dimensional Euler-Lagrange scour model — scourFoam has been developed. The model is a full three-phase (air, water and sediment) model for free-surface flow with a mobile bed. It deals with the three phases simultaneously in a natural way, which is rarely reported in scour studies. The flow field is resolved by solving the Reynolds Averaged Navier-Stokes equations using an Eulerian approach. The air-water interface is captured using a variant of the Volume of Fluid (VOF) method, which copes with the interface deformation problem in an Eulerian frame. The sediment particles are traced using the multiphase particle-in-cell method from a Lagrangian point of view. The water-sediment interface is determined using a threshold volume fraction of the sediment. Hence, the morphological development is obtained in a natural way. Drag force from the fluid, body forces and inter-particle stresses as well as the inter-phase momentum transfer are all accounted for in the model.

Navier-Stokes Equations

The Volume of Fluid method was first proposed by Hirt and Nichols (1981) for multiphase flow simulations, based on which, a modified two-fluid methodology for incompressible flows was employed to resolve the hydrodynamics of the water and air phases (Rusche, 2002). With the introduction of the volume fraction of water, α, which is bounded between 0 and 1, the momentum equation can be applied to an ensemble averaged flow velocity field. The Navier-Stokes Equations are written as,

$$\nabla \cdot \mathbf{U} = 0 \tag{1}$$

$$\frac{\partial \rho \mathbf{U}}{\partial t} + \nabla \cdot (\rho \mathbf{U}\mathbf{U}) = -\nabla p + \nabla \cdot \mathbf{T} + \rho \mathbf{F}_b \tag{2}$$

where $\mathbf{U}$ and ρ are the ensemble averaged velocity and density, respectively defined by,

$$\mathbf{U} = \alpha \mathbf{U}_w + (1 - \alpha)\mathbf{U}_a \tag{3}$$

$$\rho = \alpha \rho_w + (1 - \alpha)\rho_a, \tag{4}$$

where the subscript w and a represents the properties of water and air, respectively. p is the total pressure, which can be split into a dynamic pressure and a hydro-static component:

$$p = p_d + \rho \mathbf{g} \cdot \mathbf{x} \tag{5}$$

where $\mathbf{g}$ is the gravitational acceleration and $\mathbf{x}$ is the position vector.

$\mathbf{T}$ is the deviatoric viscous stress tensor,

$$\mathbf{T} = \mu[\nabla \mathbf{U} + (\nabla \mathbf{U})^T] - \frac{2}{3}\mu(\nabla \cdot \mathbf{U})\mathbf{I}, \tag{6}$$

where $\mathbf{I}$ is the identity matrix. As both the water phase and the air phase are treated as Newtonian and incompressible fluids, $\nabla \cdot \mathbf{U} = 0$ is satisfied. Consequently,

$$\nabla \cdot \mathbf{T} = \nabla \cdot (\mu[\nabla \mathbf{U} + (\nabla \mathbf{U})^T]) = \nabla \cdot (\mu \nabla \mathbf{U}) + (\nabla \mathbf{U}) \cdot \nabla \mu \tag{7}$$

$\mathbf{F}_b$ is the body forces per unit mass, including gravity and surface tension effects. The continuum surface force (CSF) model is employed to represent the surface tension term,

$$\mathbf{F}_b = \sigma_\kappa \nabla \alpha, \tag{8}$$

where σ_κ is the mean curvature of the free surface given by,

$$\sigma_\kappa = -\nabla \cdot \left(\frac{\nabla \alpha}{|\nabla \alpha|} \right). \tag{9}$$

Substituting Eq.5, Eq.7 and Eq.8 into Eq.2, the momentum equation reads,

$$\frac{\partial \rho \mathbf{U}}{\partial t} + \nabla \cdot (\rho \mathbf{U}\mathbf{U}) - \nabla \cdot (\mu \nabla \mathbf{U}) - (\nabla \mathbf{U}) \cdot \nabla \mu = -\nabla p_d - \mathbf{g} \cdot \mathbf{x} \nabla \rho + \sigma_\kappa \nabla \alpha \tag{10}$$

With the presence of the solid phase, a volume exclusion term (T_{ve}), which accounts for the displacement of the fluid due to particle motions, is added to the l.h.s. of the momentum equation. Following the work of Cihonski et al. (2013), it is given by,

$$T_{ve} = \rho \mathbf{U} \frac{\partial}{\partial t} ln\theta_f + \mathbf{U} \cdot \nabla (ln\theta_f), \tag{11}$$

where θ_f is the volume fraction occupied by the fluid.

The transport equation for the phase fraction α is given by,

$$\frac{\partial \alpha}{\partial t} + \nabla \cdot (\mathbf{U}\alpha) + \nabla \cdot [\mathbf{U}_r \alpha (1 - \alpha)] = 0 \tag{12}$$

where $\mathbf{U}_r$ is the relative velocity, $\mathbf{U}_r = \mathbf{U}_w - \mathbf{U}_a$. The last term on the l.h.s. of Eq.12 is an additional convective term, which is introduced for the purpose of a higher interface resolution without using additional special convection schemes. It is noteworthy that this term is applicable only within the interface region, whose thickness is theoretically infinitesimal. With the definition of α itself, this term vanishes in cells where there is purely water or purely air.

To account for the influence of the solid phase on the fluid phase, an inter-phase momentum transfer term is added to the velocity flux in Poisson equation. It is expressed by,

$$\mathbf{S}_{imt} = -\frac{1}{V_{i,j,k}} \sum_{p=1}^{np} (\rho_p V_p D_p (\mathbf{U}_f - \mathbf{U}_p)), \tag{13}$$

where $V_{i,j,k}$ is the cell volume, np is the number of particles in a cell, V_p is the volume of the particle, and D_p is a parameter related to drag coefficient.

Particle motion

The sediment particles are traced using the multiphase particle-in-cell method from a Lagrangian point of view. Following the work of Andrews and O'Rourke (1996), the Liouville equation for the particle distribution function $\phi(\mathbf{x}_p, \mathbf{U}_p, \rho_p, V_p, t)$ is introduced,

$$\frac{\partial \phi}{\partial t} + \nabla \cdot (\phi \mathbf{U}_p) + \nabla_{\mathbf{U}_p} \cdot (\phi A) = 0, \tag{14}$$

where the subscript p represent the particles, V_p is the particle volume, and A is the particle acceleration. Particle motions are governed by Newton's Law of Motion, and the particle acceleration is expressed by,

$$A = D_p(\mathbf{U}_f - \mathbf{U}_p) - \frac{\nabla p_p}{\rho_p} + (1 - \frac{\rho_f}{\rho_p})\mathbf{g} - \frac{1}{\theta_s \rho_p} \nabla \tau \tag{15}$$

where θ_s is the volume fraction occupied by the solid phase in a cell, which can be expressed by,

$$\theta_s = \int\int\int \Phi V_p dV_p d\rho_p d\mathbf{u}_p, \tag{16}$$

and τ is the inter-particle stress. Terms on the r.h.s. of Equation 15 account for the acceleration due to hydrodynamic drag, dynamic pressure gradient, net buoyant force, and inter-particle stress gradient, respectively, which are all taken into consideration in the model. The inter-particle stress gradients are usually computed in an Eulerian sense, which exert the maximum packing fraction limit to each cell.

The parameters involved in the hydraulic drag term read (Andrews and O'Rourke, 1996),

$$D_p = C_d \frac{3}{8}\frac{\rho_f}{\rho_p}\frac{|\mathbf{U}_f - \mathbf{U}_p|}{r_p} \tag{17}$$

$$C_d = \frac{24}{Re_p}(\theta_f^{-2.65} + \frac{1}{6}Re_p^{2/3}\theta_f^{-1.78}), \tag{18}$$

$$Re_p = \frac{2\rho_f|\mathbf{U}_f - \mathbf{U}_p|r_p}{\mu_f} \tag{19}$$

where the fluid volume fraction θ_f is calculated by $\theta_f = 1 - \theta_s$.

When the solid volume fractions are above 5%, frequent particle collision will take place, and for dense particulate flows in the Eulerian-Lagrangian approach, it is not suitable to use Lagrangian collision calculations to represent the inter-particle stress due to collision (Patankar and Joseph, 2001). Therefore, continuum models are considered here.

A continuum particle stress model (Snider, 2001), which is extended from the model by Harris and Crighton (1994), is employed here. In this model, particles are treated as a continuum with an assumption of an isotropic inter-particle stress where the off-diagonal elements of the stress tensor are omitted. The particle normal stress is modelled by a continuum calculation of the particle pressure, which will then be interpolated back to discrete particles' position to calculate the normal stress due to motion and inelastic collision of particles. The model is given by,

$$\tau = \frac{P_s\theta_s^\beta}{max[\theta_{sm} - \theta_s, \varepsilon(1-\theta_s)]}, \tag{20}$$

where the constant P_s is of the unit of pressure, β is a constant in the range $2 \le \beta \le 5$, and θ_{sm} is the solid volume fraction at maximum packing. A small number ε of the order 10^{-7} was introduced by Snider (2001) to remove the spikes at close pack. Obviously, this model depends only on the solid volume fraction, and particle size and velocity are excluded. Though it is a simple model, it has been widely employed and proven to be efficient in dense particle flows (Snider, 2001; Patankar and Joseph, 2001).

The particle velocity is updated in two stages. Firstly, the particle velocity updated by forces excluding inter-particle stress force is calculated; secondly, the particle velocity change due to inter-particle stress is calculated and added to the velocity obtained in the first stage.

The integrated form of Eq.15 excluding the inter-particle stress term can be written as,

$$\mathbf{u}_{p1}^{n+1} = \frac{\mathbf{u}_p^n + \Delta t D_p \mathbf{u}_{f,p}^{n+1} - \frac{\Delta t}{\rho_p}\nabla p_p^{n+1} + \Delta t(1 - \frac{\rho_f}{\rho_p})\mathbf{g}}{1 + \Delta t D_p}, \tag{21}$$

where $\mathbf{u}_{f,p}^{n+1}$ is the fluid velocity interpolated at the particle location. The velocity change due to inter-particle stress is given by,

$$\mathbf{u}_{p2}^{n+1} = -\frac{\Delta t \nabla \tau}{\rho_p \theta_s(1 + \Delta t D_p)}. \tag{22}$$

The particle velocity updated in the above two stages is then summed up to get the velocity at new time step,

$$\mathbf{u}_p^{n+1} = \mathbf{u}_{p1}^{n+1} + \mathbf{u}_{p2}^{n+1}. \tag{23}$$

The particle positions are updated by

$$\frac{D\mathbf{x}_p}{Dt} = \mathbf{U}_p \tag{24}$$

The water-sediment interface is determined using a threshold volume fraction of the sediment. Hence, the morphological development is obtained in a natural way.

RESULTS AND DISCUSSIONS

Steady current test

The experiment of steady current case was carried out by Sumer et al. (1997) in a wave flume with a length of 26.5 m, a width of 0.6 m and a depth of 0.8 m. The water surface was maintained at 0.4 m constantly. A vertical cylinder with a diameter of 0.04 m was placed in the flume. The incoming velocity was 9.5 cms^{-1}.

The mesh used in the model is 0.8 m long, 0.6 m deep, and 0.4 m wide, which are 20 times, 15 times and 10 times of the pile diameter respectively, to avoid the blockage effect. There are 100, 50 and 50 cells in the x, y, and z direction, respectively. Note that $y-axis$ is the vertical axis. The grid around the pile and near the bed is refined. As the flow is in turbulent regime, $k-\varepsilon$ turbulence model is employed.

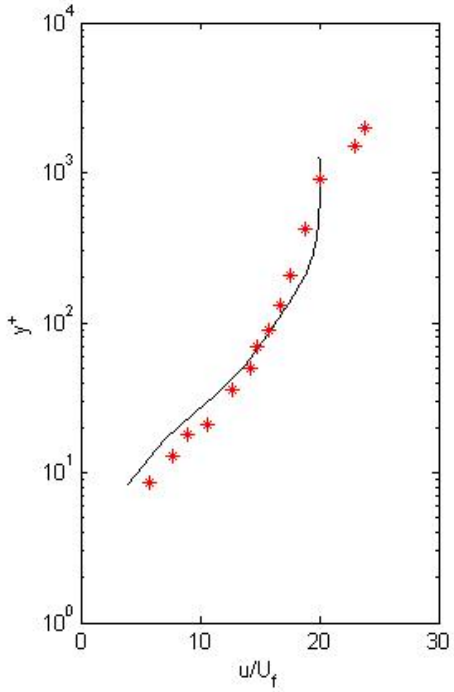

Figure 1: Velocity profile in the steady current case. Solid line, modelling results; symbols, experimental measurements.

The modelled velocity profile in comparison with the measurements is presented in Figure 1. $y^+ = yU_f/\nu$, where U_f is the friction velocity and ν is the kinematic viscosity of water. Overall, the modelling results agree well with the measurements, whereas the velocity near the free surface or the bed is under-predicted. This may require a finer mesh resolution, especially around the cylinder circumference and near the bed. However, as the mesh is three-dimensional, it is challenging to generate a mesh fine enough to resolve very detailed flow structures, while the domain remains large enough to avoid blockage effect.

Rough rigid bed test

In the rough rigid bed test carried out by Roulund et al. (2005), a vertical pile with the diameter D being 0.536 m was placed on a rough bed. The bed roughness height $k = 0.7\,cm$. For the numerical model, the computing domain is 5 m long, 1 m deep, and 3 m wide, consisting of 160, 45 and 112 cells in each

direction, respectively. Finer mesh is constructed around the pile and near the bed. The water depth is kept at 0.54 m. The inlet velocity is 0.326 ms^{-1}. The $k-\varepsilon$ turbulence model is employed in this case.

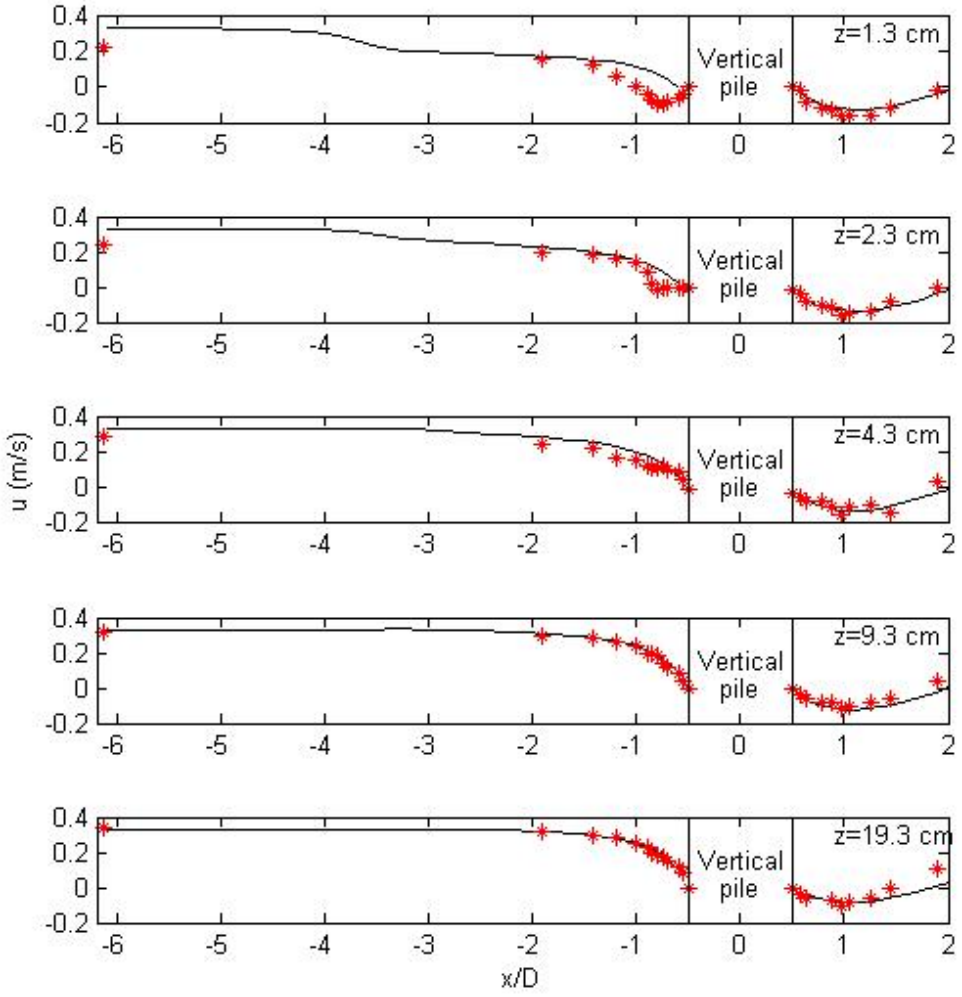

Figure 2: Horizontal velocity in the plane of symmetry at different vertical layers. z is measured from the bed. Solid line, modelling results; symbols, measurements.

The horizontal velocity at different vertical layers at the plane of symmetry is presented in Figure 2. Very good agreement between the modelling results and the experimental measurements is achieved, especially in the downstream side of the cylinder. In the upstream side, the predicted velocities at layers 4.3 cm above the bed and higher match with the experimental results well. In addition, velocity deacceleration at each layer in the upstream side starts at different distances from the inlet. Horizontal velocity deacceleration starts earlier at layers close to the bed as expected, approximately $5D$ ahead of the vertical cylinder, and it occurs only $2D$ ahead of the cylinder at the layer near the free surface. This demonstrates the real three-dimensional feature of the model. However, Some discrepancies near the pile at the upstream side are observed in the layers very close to the bed, i.e., $z = 1.3\,cm$ and $z = 2.3\,cm$.

Nevertheless, the good performance overall confirms the ability of the model to simulate three-dimensional flow around vertical cylinders in steady currents. A high-accuracy prediction of the hydrodynamics is a pre-

requisite to a reasonable prediction of scour.

Pipeline scour test

The clear-water experiments with a horizontal pipeline above an erodible bed by Mao (1986) have been a benchmark test for scour models. The pipeline diameter is $0.1\,m$. The water level is maintained at $0.4\,m$. A two-dimensional mesh ($1.35\,m$ long and $0.6\,m$ deep) was constructed with a resolution of $0.25\,cm$. The inlet velocity is $0.35\,m/s$. The bed is flat initially, without any manual introduction of bed profiles such as sinusoidal profile.

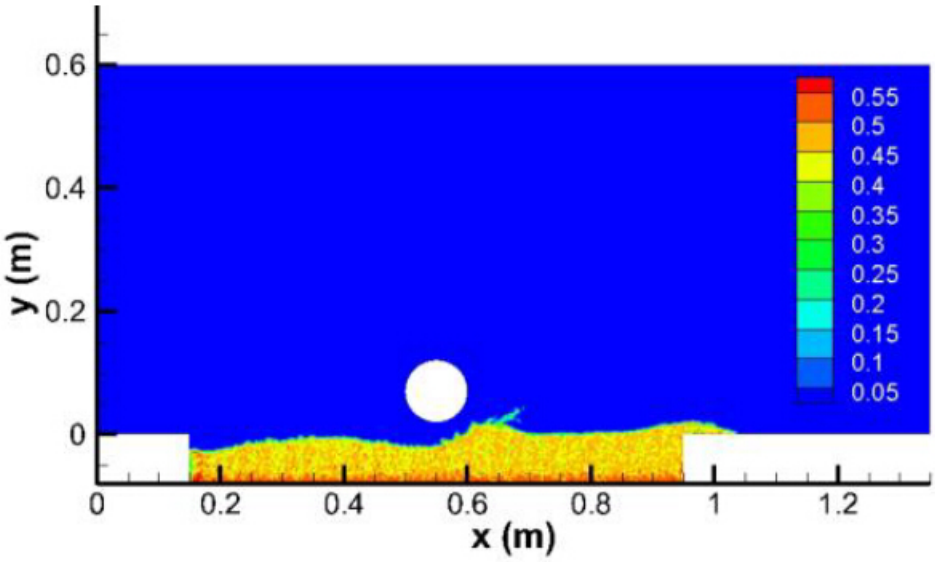

Figure 3: Solid volume fraction in the pipeline scour test.

Figure 3 shows the solid volume fraction in this pipeline scour test. The bed profile is extinguished from the flow domian by the isoline of a threshold value of solid volume fraction. In Figure 4, the development of the fluid velocity field at different time and bed profile evolution are shown. Obviously, the fluid phase feels the presence of particles and the pipeline. Flow contraction and acceleration are well resolved around the pipeline and in the gap above the bed. Lee-wake vortex and vortices shedding are captured by the model. As we can see, scattering events happen at the very beginning of the scour process. Particle entrainment takes place and particles flow with the fluid phase towards the downstream side. From $16\,s$ onwards, less events-dominated process is observed. The dune formed by the deposition of sediments continues moving downstream and the maximum scour location evolves to the upstream side slightly. The capability of the scour model is therefore well demonstrated.

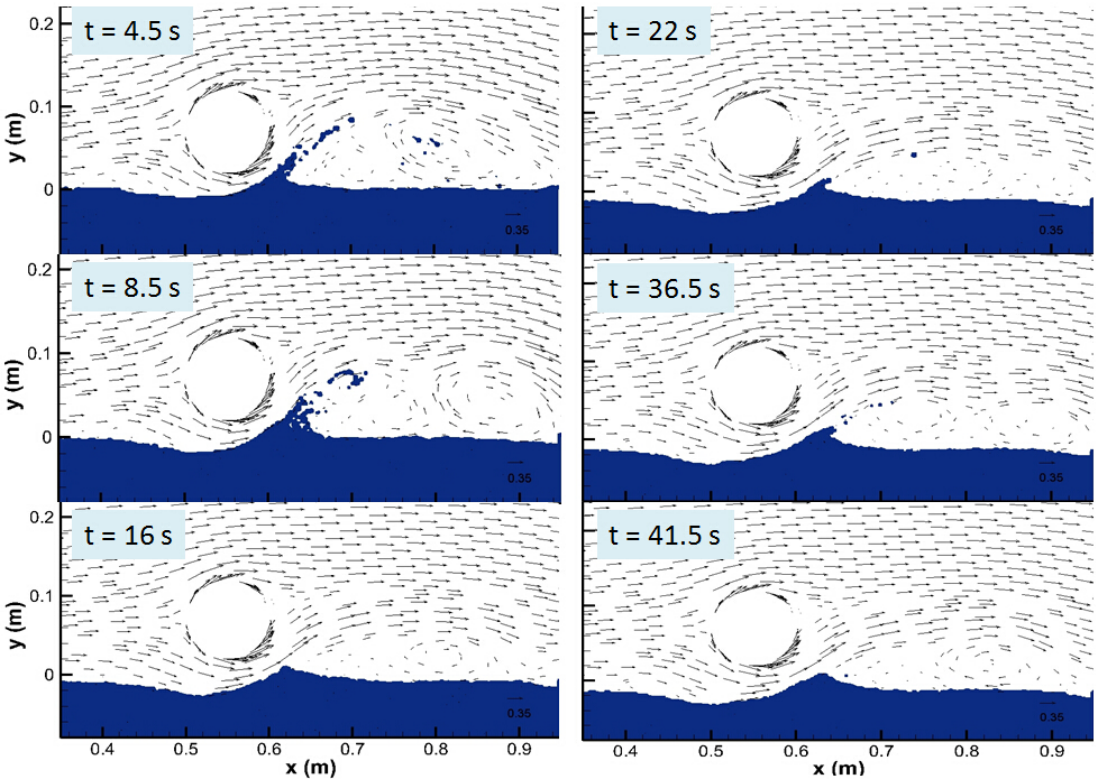

Figure 4: Bed profile evolution and the development of the fluid velocity field in the pipeline scour test.

CONCLUSIONS

In this work, a full three-phase, hybrid Eulerian-Lagrangian scour model for free-surface flow with a mobile bed has been developed. It retains the inherent physical properties of each phase while being computationally efficient. The hydrodynamics in the presence of vertical and horizontal cylinders are resolved well and vortices on the wake side of the cylinder are captured.

Scour development at the beginning is largely dominated by scattering events. The model successfully captured such events as avalanching without the ad-hoc parametrization required by continuum models. The interaction between the fluid phase, solid phase and the structures appears to be well represented by the model. Moreover, the model is able to predict the onset of scour under a cylinder from an initially flat bed.

ACKNOWLEDGEMENTS

The authors would like to thank HR Wallingford, and Engineering and Physical Sciences Research Council (EPSRC) for their generous funding to this research.

References

M. Andrews and P. O'Rourke. The multiphase particle-in-cell (mp-pic) method for dense particulate flows. *International Journal of Multiphase Flow*, 22(2):379 – 402, 1996. ISSN 0301-9322. doi: http://dx.doi.org/10.1016/0301-9322(95)00072-0.

A. Cihonski, J. Finn, and S. V. Apte. Volume displacement effects during bubble entrainment in a travelling vortex ring. *Journal of Fluid Mechanics*, 721:225–267, 2013. doi: 10.1017/jfm.2013.32.

S. E. Harris and D. G. Crighton. Solitons, solitary waves, and voidage disturbances in gas-fluidized beds. *Journal of Fluid Mechanics*, 266:243–276, 5 1994. ISSN 1469-7645. doi: 10.1017/S0022112094000996.

C. Hirt and B. Nichols. Volume of fluid (vof) method for the dynamics of free boundaries. *Journal of Computational Physics*, 39(1):201 – 225, 1981. ISSN 0021-9991. doi: 10.1016/0021-9991(81)90145-5.

F. Li and L. Cheng. A numerical model for local scour under offshore pipelines. *J Hydr Eng*, 125:400–406, 1999.

F. Li and L. Cheng. Numerical simulation of pipeline local scour with lee-wake effects. *Int J Offshore Polar Eng*, 10:195–199, 2000.

D. Liang, L. Cheng, and K. Yeow. Numerical study of the reynolds-number dependence of two-dimensional scour beneath offshore pipelines in steady currents. *Ocean Engineering*, 32(13):1590 – 1607, 2005. ISSN 0029-8018. doi: 10.1016/j.oceaneng.2004.10.025.

Y. Mao. *The Interaction Between a Pipeline and an Erodible Bed*. Institute of Hydrodynamics and Hydraulic Engineering København: Series paper. Institute of Hydrodynamics and Hydraulic Engineering, Technical University of Denmark, 1986.

N. Patankar and D. Joseph. Lagrangian numerical simulation of particulate flows. *International Journal of Multiphase Flow*, 27(10):1685–1706, 2001. doi: doi:10.1016/S0301-9322(01)00025-8.

RenewableUK. URL `http://www.renewableuk.com/en/renewable-energy/wind-energy/offshore-wind/`.

A. Roulund, B. M. Sumer, J. Fredsøe, and J. Michelsen. Numerical and experimental investigation of flow and scour around a circular pile. *Journal of Fluid Mechanics*, 534:351–401, 6 2005. ISSN 1469-7645. doi: 10.1017/S0022112005004507.

H. Rusche. *Computational fluid dynamics of dispersed two-phase flows at high phase fractions*. PhD thesis, Imperial College, University of London, 2002.

D. Snider. An incompressible three-dimensional multiphase particle-in-cell model for dense particle flows. *Journal of Computational Physics*, 170(2):523–549, July 2001.

D. Snider, P. O'Rourke, and M. Andrews. An incompressible two-dimensional multiphase particle-in-cell model for dense particle flows. La–13280-ms, Los Alamos National Lab., NM (United States), June, 1997.

B. Sumer and J. Fredsøe. *The Mechanics of Scour in the Marine Environment*. Advanced Series on Ocean Engineering. World Scientific, 2002. ISBN 9789810249304.

B. Sumer, N. Christiansen, and J. Fredsøe. The horseshoe vortex and vortex shedding around a vertical wall-mounted cylinder exposed to waves. *Journal of Fluid Mechanics*, 332:41–70, 1 1997. ISSN 1469-7645.

A. Yeganeh-Bakhtiary, M. H. Kazeminezhad, A. Etemad-Shahidi, J. H. Baas, and L. Cheng. Euler-euler two-phase flow simulation of tunnel erosion beneath marine pipelines. *Applied Ocean Research*, 33(2): 137 – 146, 2011. ISSN 0141-1187. doi: 10.1016/j.apor.2011.01.001.

M. Zhao and L. Cheng. Numerical investigation of local scour below a vibrating pipeline under steady currents. *Coastal Engineering*, 57(4):397 – 406, 2010. ISSN 0378-3839. doi: 10.1016/j.coastaleng.2009.11.008.